

Mice's Liver, Kidney, and Suprarenal Gland Histogenesis Mus Musculus

Dina H. Sadiq

Basic Sciences Department, College of Nursing, University of Basrah, Basrah, Iraq

Email: dinahamid234@gmail.com

Abstract. This work used histological and histochemical methods to look at how the mice's liver, kidney, and suprarenal glands develop after birth. Therefore, using mice in scientific research is permissible. The experiment used thirty-two samples of the liver, kidney, and suprarenal gland of mice, eight at each age (one day, seven days, fourteen days, and twenty-one days). A thin capsule encased the liver on the first day of life; a thicker capsule encased it after 14 to 21 days. Hepatocytes made up the parenchyma, and a central vein encircled them. The parenchyma was further split by the sinusoids, and Next to the endothelial cells that encircled the hepatic sinusoids were protruding Kupffer cells. The liver measurements change with aging. Cortical, midcortical, and juxtamedullary renal corpuscles are distinguished by their increasing diameter with age. Distal convoluted tubules are shorter than the longest convoluted tubules, which are the proximal ones. Furthermore, Henle loops were short at one-day and adult ages but long at other ages.

Highlights:

1. Postnatal development of liver, kidney, and adrenal glands showed significant age-dependent structural changes in mice.
2. Renal corpuscles increased in diameter with age, while Henle loops were short at 1 day and adulthood but elongated at intermediate stages.
3. Histochemical analysis revealed well-developed basement membranes and tubular structures, indicating progressive organ maturation.

Keywords: Mice, Liver, Kidney, Suprarenal Gland, Histogenesis, Mus Musculus

Introduction

Two distinct embryological structures give rise to the adrenal glands [1]. The combination of intracellular and extracellular signals preserves the integrity and function of the

adrenal glands. This regulation depends on adrenocorticotrophic hormone (pituitary hormone), the main hormone that stimulates the generation and secretion of adrenal glucocorticoids. Basic and clinical researchers are interested in. Given the substantial advancements in our understanding of the anatomy of the embryonic process and the adrenal gland's extraordinary ability for regeneration, it is important to learn the mechanisms underpinning growth, development, upkeep, and regeneration of the adrenal glands [2]. Hepatocytes in the liver lobes originate in the central alimentary canal, split by circulation channels, and eventually spread into sinusoids [3-8].

The development of the pronephros, mesonephros, and metanephros, a more advanced pair of kidneys, distinguishes the three phases of kidney development in mammals [9]. The initial stage of the mesonephric nephron's formation is the mesenchymal condensation. These condensates rapidly form renal vesicles and S-shaped structures. The metanephros has been shown to go through comparable developmental phases. The different nephron segments' mesenchymal origins are separated by the Wolffian duct and the collecting duct [10-13]. Domestic animals have large, firm kidneys that resemble beans [14]. This makes it possible for it to find a vast amount of information while using search engines to look up any topic, whether at home or at work [15].

Materials and Methods

Ethical Consideration

From March to May 2024, all procedures were completed in compliance with the University of Baghdad, Iraq, animal care norms.

Study animals: An investigation including thirty-two mouse samples of the kidney, liver, and suprarenal gland was carried out between March and May of 2024. A newborn was represented by a mouse that was one day old, a nursing mouse by seven days, a weaning mouse by fourteen days, and an adult mouse by twenty-one days.

Collection of Samples

All ages, except one day, are put into anesthesia by administering an injection of ketamine. Each animal's ventral abdominal wall had its kidney, liver, and adrenal (suprarenal)

Indonesian Journal on Health Science and Medicine Vol 1 No 2 (2025): October

ISSN 3063-8186. Published by Universitas Muhammadiyah Sidoarjo Copyright ©
Author(s). This is an open-access article distributed under the terms of the Creative
Commons Attribution License (CC-BY).
<https://doi.org/10.21070/ijhsm.v1i2.286>

glands removed. The visceral organs had been removed, and the midline of the abdomen had been cut. The research was subjected to histopathological examination [16].

Technique of Histological: Microtome sectioning, paraffin wax infiltration and embedding, xylene washing, and ethanol alcohol dehydration [16].

Tissue staining: The stains that were utilized were Masson's trichrome, Mallory, Verhoeff's, and hematoxylin and eosin (H @ E) [17].

Staining of Histochemical

Sections were immersed in an aqueous solution containing 1% periodic acid for thirty minutes. The slices were cleansed to get rid of any remaining acid after being exposed to Schiff's reagent for twenty minutes and potassium metabisulfite 0.55% for one minute. Two-point five pH of alcian blue: To create acidic mucopolysaccharides, follow these steps: To deparaffinize the substance, use xylene. Rehydrate in graded ethanol following ten minutes with Nuclear Fast Red, five minutes with tap water, and thirty minutes with Alcian Blue. Use the water for a minute. Neutral and acidic mucopolysaccharides were then compared in order to attain dehydration. Alcian blue; pH 2.5; microwave. Give yourself two to five minutes to stand and forty-five seconds to apply your utmost force. Rinse with distilled water after washing under the faucet for approximately five minutes. Work with 0.5% periodic acid for five minutes. When washing, use de-ionized water. Use Schiff's Reagent and the microwave to recuperate for two to five minutes following forty-five seconds of vigorous exertion [17].

Statistical Analysis

The study was examined at the 5% significance level using the one-way analysis of variance (ANOVA) test. Statistical software for social science was used to handle and analyze the data [18].

Results and Discussion

The adrenal gland is composed of the cortex and medulla. The cortex is surrounded by the mesenchymal cells that comprise the adrenal capsule. Because they control the endocrine system, the three separate cortical zones beneath the capsule—the innermost zona reticularis, the middle zona fasciculata, and the outermost zona glomerulosa—are critical to an organism's

lifespan, despite their disparate roles and developmental genesis (Fig. 1-4) [19]. Explain the descent of the adrenal glands after their peritoneal development. The adrenal cortex produces steroid hormones from cholesterol through a variety of biological metabolic mechanisms. The medulla, a component of the sympathetic nervous system, is in charge of manufacturing adrenaline and norepinephrine [20]. The developmental program of the adrenal gland starts in the embryo and continues through the fetus and postnatal animals [2]. The adrenal gland undergoes significant reorganization during the postnatal phase. Soon after birth, the cells of the zona fasciculata undergo apoptosis, causing the remaining zona fasciculata to involute. Conversely, the growth hormones angiotensin II and ACTH cause the maturation of the adult zona glomerulosa and zona fasciculata. The adrenal zona reticularis then develops between the zona fasciculata and medulla, and is characterized by increased adrenal androgen production and proliferation. The remaining sections of the mouse's X-Zone, or zona fasciculata, eventually retreat when puberty starts in rodents [21].

values that are lower on the first day of life than at subsequent ages are among the age-related differences in adrenal layer thickness (Table 1). Through the release of steroid hormones, the adrenal cortex regulates a number of physiological processes, including energy metabolism, salt metabolism, and stress response. As a mineralocorticoid, aldosterone secretion needs to be carefully regulated and tailored to the body's needs. In the outermost layer of the adrenal cortex, the two primary stimulants of aldosterone generation and release are angiotensin II. Since aldosterone stimulates the kidneys to release K⁺ and reabsorb Na⁺, it is crucial for controlling blood pressure and the makeup of plasma electrolytes [1].

Angiotensinogen is converted by renin to angiotensin I, which is subsequently changed by an angiotensin-converting enzyme in the lung to angiotensin II. This causes primary cells to excrete more potassium, intercalated collecting duct cells to excrete more hydrogen ions, and sodium reabsorption to increase. The zona fasciculata cells are responsible for producing glucocorticoids. The majority of glucocorticoids, including cortisol, which can mobilize lipids, proteins, and carbohydrates, are normally produced by the adrenal cortex. The main glucocorticoid produced and utilized by mice and rats is corticosterone [21].

Indonesian Journal on Health Science and Medicine Vol 1 No 2 (2025): October

ISSN 3063-8186. Published by Universitas Muhammadiyah Sidoarjo Copyright ©
Author(s). This is an open-access article distributed under the terms of the Creative
Commons Attribution License (CC-BY).
<https://doi.org/10.21070/ijhsm.v1i2.286>

From birth, the kidneys of mice continuously enlarge, and after seven days, they exhibit further morphogenesis. Different levels of glomerular condensation were found in the renal cortex's cortical and subcortical zones; the periphery grew faster than the mid-cortical and subcortical zones. The cortical and subcortical areas of the kidney have a greater number of renal corpuscles than the juxtamedullary zones. The corpuscles displayed Bowman's capsules and a discernible parietal squamous layer. More development was observed in the distal convoluted tubules as well as the proximal ones. At this age, the medulla had nuclei in the middle, cuboidal epithelium surrounding the collecting duct, clear intercellular membranes, and cytoplasm that was faintly pigmented (Fig. 5,6). This aligns with a study [22], According to this, kidneys develop in the pelvis and rise [3]. Thus, variations in tubule activity related to water quality were associated with this. Furthermore, delicate secretions were loaded into proximal tubules in order to enhance the tubule lumen's surface area, recover more lumen components into the circulation, and increase the amount of fluid consumed. The proximal tubule cells also absorb almost all nutrients [23].

By day fourteen, the kidney's morphogenesis and renal structure establishment had improved. The parietal squamous layer and Bowman's capsules were clearly apparent. By the end of this period, each component of the nephron has developed into a unique histology. The Henle loops are plainly evident, and the proximal convoluted tubule epithelium has a well-developed brush border. The renal pyramids in the medulla as they ascended into the subcortical and cortical zones. The renal papilla, encircled by low cuboidal epithelium in collecting tubules, arises when the medullary pyramid's circular peak drops from the base (Fig. 7-11). This is analogous to research [24].

The renal parenchyma structure of 21-day-old mice's kidneys was found to be fully formed. Collagen fibers, which comprise a significant amount of the stroma, are found in the interstitial tissue capsule. It was found that the characteristic Bowman's gap around the glomeruli is the source of the proper morphology of renal corpuscles. Differentiation is shown by the lining cells of the proximal tubules' characteristic eosinophilic cytoplasm. The denser medulla contained collecting tubules, ducts, and renal loop elongation. A capsule of collagenous fibrous tissue encloses the kidney in adults (Figures 5-11). A substantial difference

($P > 0.05$) was seen in the adult kidney's thickness and blood flow, which is responsible for cleaning the blood in circulation, compared to other ages (Table 1). These warnings resembled a study [25].

In the current work, kidney size and shape were controlled based on the animal's age using a connective tissue capsule. At different phases of embryonic development, the glomerulus was situated subcapsularly and seems to have entered Bowman's capsule through invagination (Fig. 10). The Bowman's gap shifted [26], which offered confirmation of this. According to the current study, an adult mouse's kidney at 21 days of life has the typical characteristics of an adult nephron. The juxtaglomerular apparatus, which is composed of large lumen distal tubules that are located near the renal corpuscles' vascular pole, contains podocytes that are evident around the glomerulus (Fig. 10,11). This aligns with the results of a study [27]. The macula densa cells send chemical signals that cause the renin enzyme to be released into the bloodstream. These are vasoconstrictor cells, which respond very well to both the ion concentration and the fluid volume in the tube. During these procedures, mesangial cells perform phagocytic tasks [27].

Compared to other age groups, adulthood has more noticeable age-related changes in the thickness of the hepatic duct, hepatic artery, and central vein. The liver showed faster morphogenesis and hepatic cell structure development at 30 days of life. A few connective tissue septa divide the liver's lobules. The core veins are surprisingly found inside the lobules. The spherical nuclei of polyhedral hepatocytes were arranged in irregular cords. The hepatic artery, bile duct, and the portal triads, which are located in the angles of the hepatic lobules, are branches of the portal vein (Figures 14-16). Research indicates that compared to livers of various ages, the portal triad of the adult liver is wider [26]. Increased hepatocyte and metabolic activity, which aid in maintaining body homeostasis and are connected to age-related changes in surface area and size, could be the cause of this. Numerous investigations into the liver, environment, and embryonic development have discovered that these Animals' adaptation to their surroundings demonstrates how several factors influence the liver's form [4]. In order to provide a protective physiological role, when harmful compounds and foreign objects enter through the portal artery, they are absorbed by Kupffer cells [26].

Indonesian Journal on Health Science and Medicine Vol 1 No 2 (2025): October

ISSN 3063-8186. Published by Universitas Muhammadiyah Sidoarjo Copyright ©
Author(s). This is an open-access article distributed under the terms of the Creative
Commons Attribution License (CC-BY).
<https://doi.org/10.21070/ijhsm.v1i2.286>

Histochemical studies revealed that the cells of the kidney, liver, adrenal cortex, and adrenal medulla all responded favorably to PAS, AB, and PAS-AB. PAS stain revealed the well-developed basement membranes of the glomerulus as well as the brush boundary of the proximal tubules. In the renal cortex, where the renal tubules encircled the renal corpuscle, the mature structure of the renal components was seen [2, 8, 26]. The glomerulus basement membranes and renal tubules were stained with PAS (Figures 1, 2, 6, 9, 10).

Table 1: Kidney and adrenal gland measurements, in μm ($\bar{X} \pm \text{S.E.}$)

Species Part	The adrenal glands' capsule	The Cortex	The medulla	Kidney capsule	glomerulus	Proximal tubules	the distant tubules
1 day	24.6 \pm 0.1 B	901.1 \pm 1.2 B	102.3 \pm 0.04 B	37.7 \pm 2.3B	122.4 \pm 0.3 b	74.3 \pm 0.02 B	32.2 \pm 0.01 B
7 days	26.3 \pm 0.4 B	915.2 \pm 1.6 B	112.5 \pm 0.06 B	40.5 \pm 1.5B	127.5 \pm 0.2 b	83.2 \pm 0.01 B	39.4 \pm 0.02 B
14 days	30.1 \pm 0.2 B	924.4 \pm 1.4 B	122.3 \pm 0.07 B	43.2 \pm 0.5B	132.6 \pm 0.1 b	88.5 \pm 0.04 B	42.2 \pm 0.07 B
21 days	33.5 \pm 0.6 B	932.6 \pm 1.5 B	127.2 \pm 0.04 B	47.6 \pm 2.3B	139.7 \pm 0.2 b	97.2 \pm 0.03 B	53.1 \pm 0.02 B

Table 2: Liver measurements at various ages, expressed in μm ($\bar{X} \pm \text{S.E.}$)

Measure Age	Capsule	Central vein	Hepatic duct
1 day	67.1 \pm 0.3 B	531.4 \pm 2.4 B	239.1 \pm 0.4 B
7 days	73.4 \pm 1.5 B	550.5 \pm 1.1 B	255.8 \pm 0.6 B
14 days	103.6 \pm 0.1 B	582.3 \pm 2.3 B	252.7 \pm 0.5 B
21 days	132.4 \pm 1.2 B	625.1 \pm 2.7 B	260.2 \pm 0.3 B

A significant difference ($P > 0.05$) is indicated by values in the same column that are capitalized, whereas nonsignificant differences ($p < 0.05$) are shown by values in the same column that are tiny.

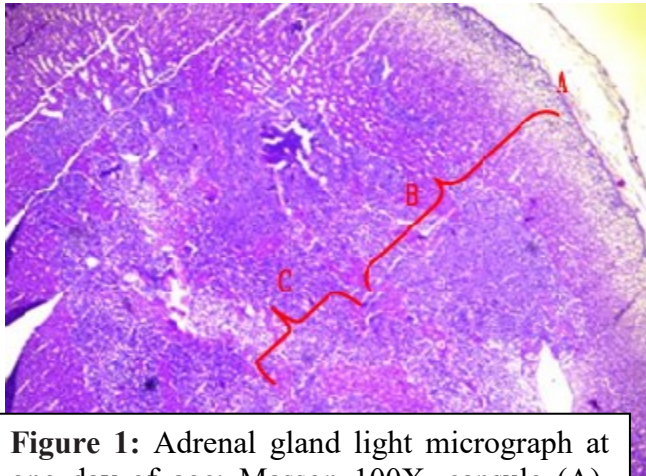


Figure 1: Adrenal gland light micrograph at one day of age; Masson 100X, capsule (A), cortex (B), and medulla (C).

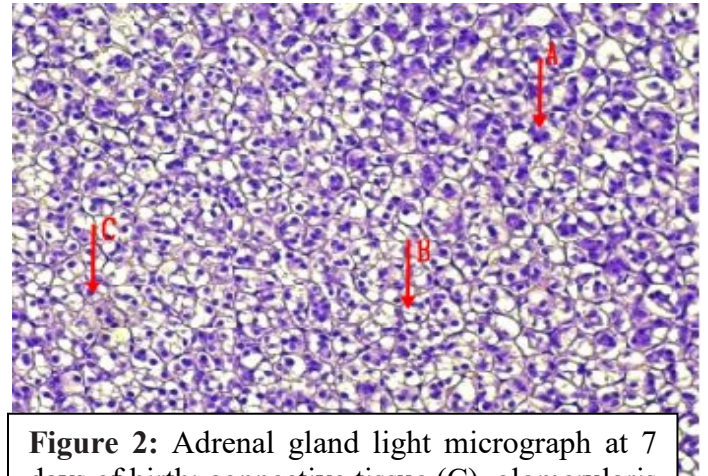


Figure 2: Adrenal gland light micrograph at 7 days of birth; connective tissue (C), glomerularis cells (A), and fascicularis cells (B), PAS 200X

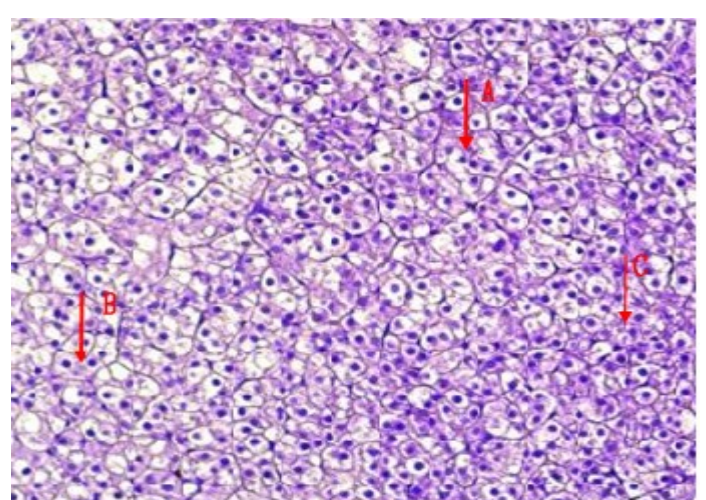
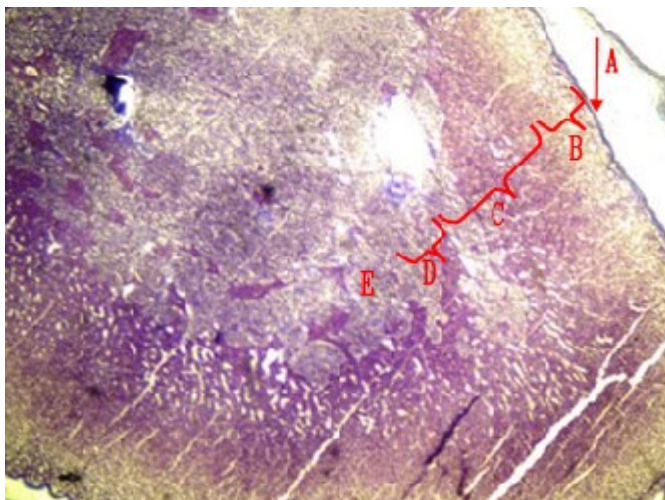


Figure 3: Mallory 100X, the medulla (E), reticularis (D), fascicularis (C), glomerularis (B), and capsule (A) are all visible in this Adrenal gland light micrograph on day 14.

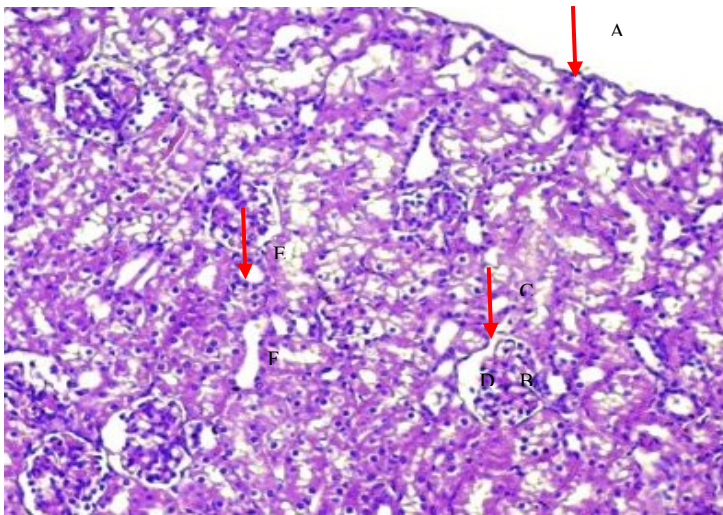


Figure 4: Adrenal gland light micrograph at 21 days of life; connective tissue (C), fascicularis cells (B), and glomerularis cells (A), AB 200X.

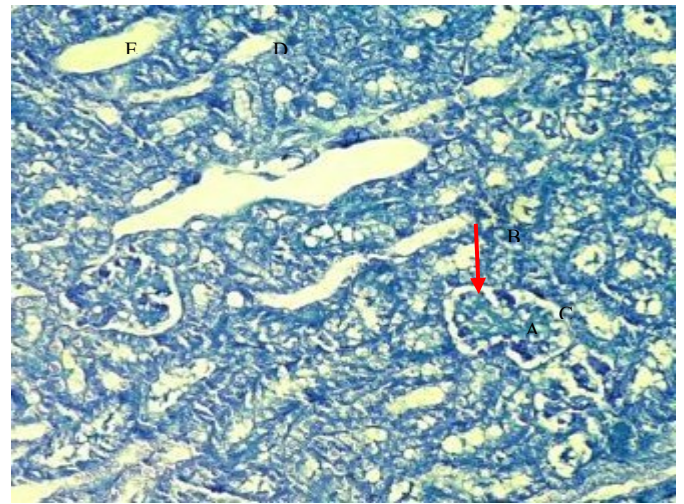


Figure 5: Kidney light micrograph at 1 day of age: PAS-AB 200X, proximal tubule (E), distal tubule (F), renal space (D), glomerulus (B), Bowman capsule (C), and capsule (A).

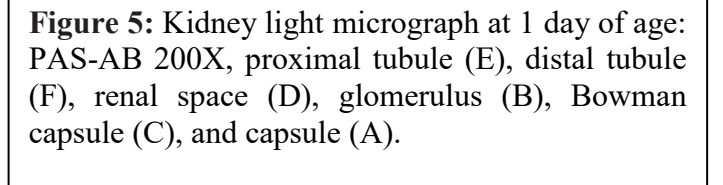
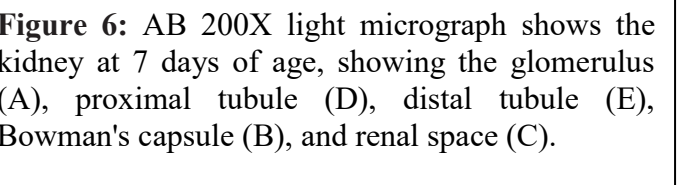


Figure 6: AB 200X light micrograph shows the kidney at 7 days of age, showing the glomerulus (A), proximal tubule (D), distal tubule (E), Bowman's capsule (B), and renal space (C).



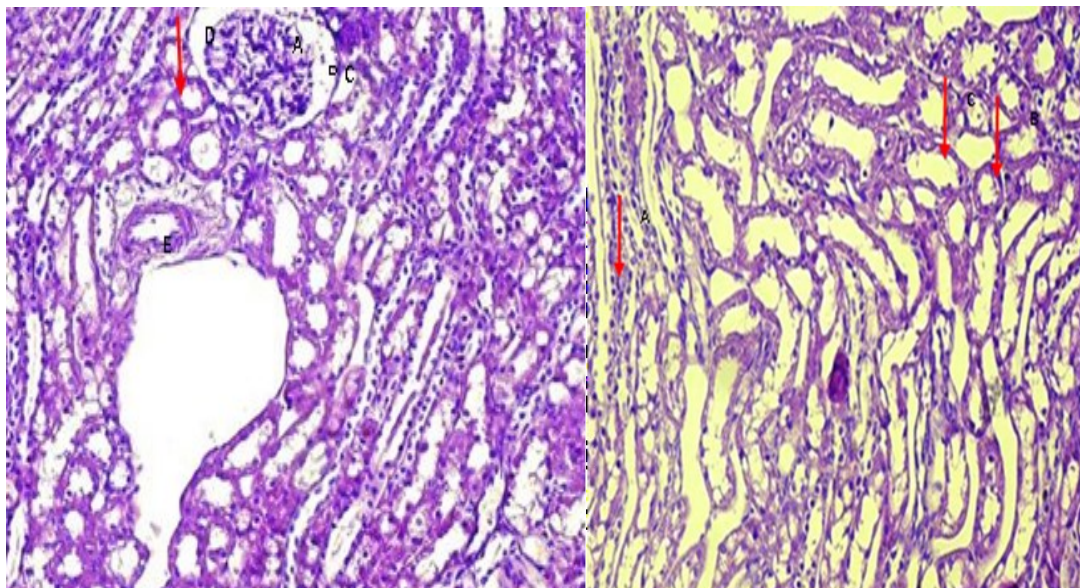


Figure 7: Kidney light micrograph at 14 days of age: blood vessels (E), juxtaglomerular apparatus (D), PAS-AB 200X, glomerulus (A), renal space (B), and Bowman's capsule (C).

Figure 8: kidney light micrograph at 21 days of life; AB 200X, proximal tubule (B), distal tubule (C), and loop of Henle (A).

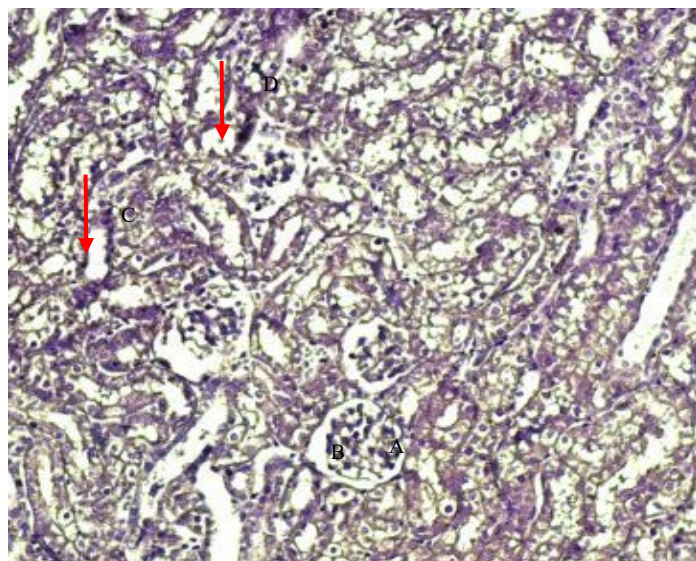


Figure 9: At 7 days of age, the proximal tubule (C), distal tubule (D), and renal space (B), and glomerulus (A) of the kidney are visible in this Mallory 200X light micrograph.

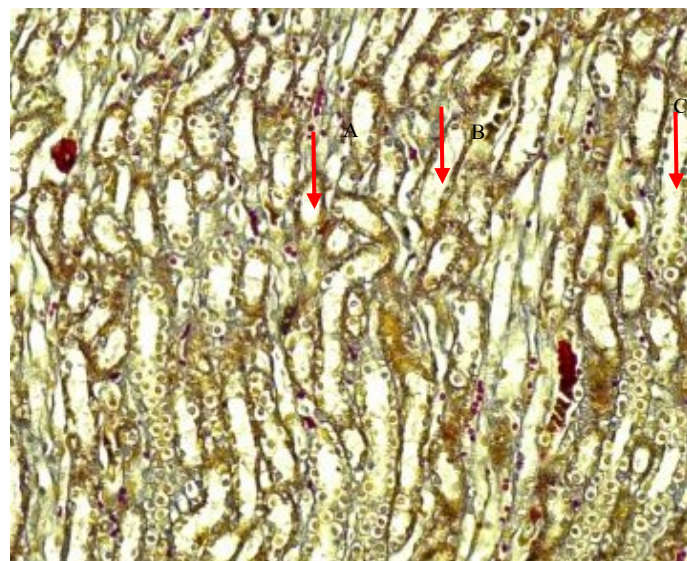


Figure 10: The kidney's light micrograph at 14 days of age shows the Henle loop (C), proximal and distal tubules (A and B), and Verhoeff 200X.

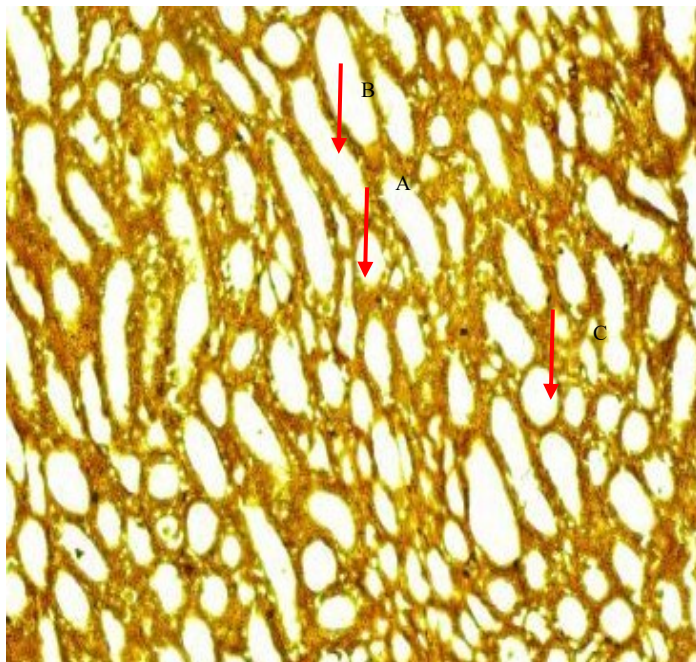


Figure 11: Verhoeff's 200X light micrograph of the kidney at 21 days of age, showing the collecting duct (C), proximal tubule (A), and distal tubule (B).

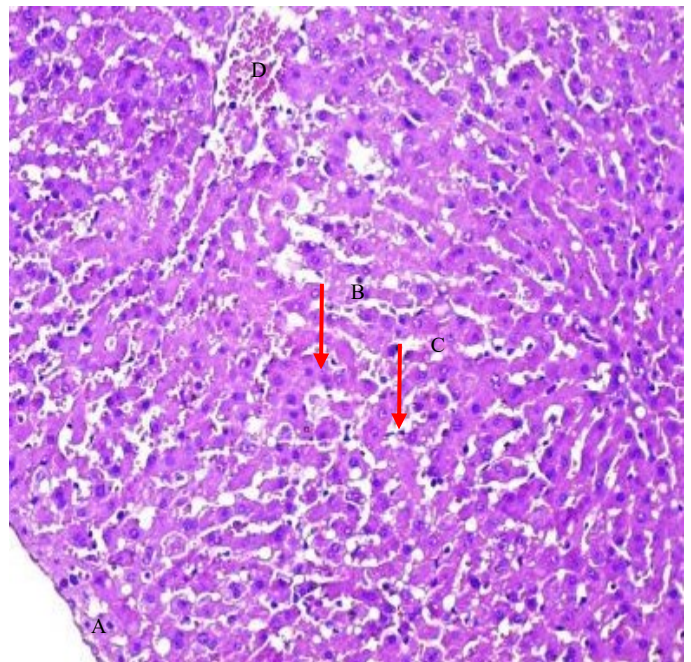
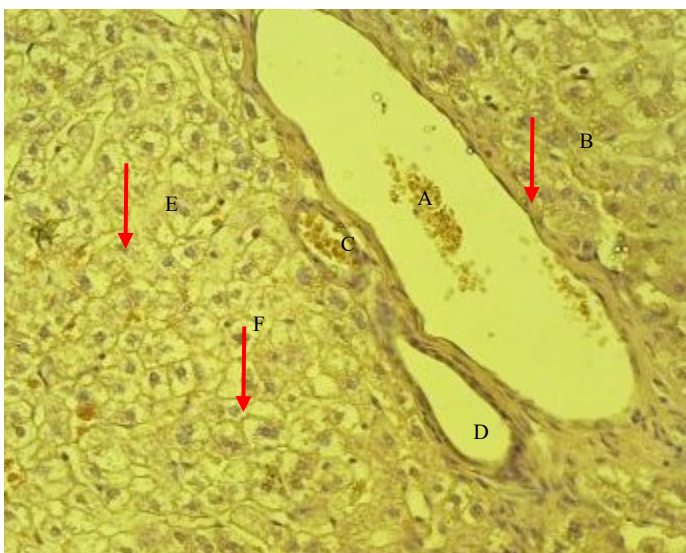


Figure 12: A day-old liver light micrograph showing the central vein (D), sinusoids (C), hepatic cells (B), and capsule (A) at H&E 200X.



1

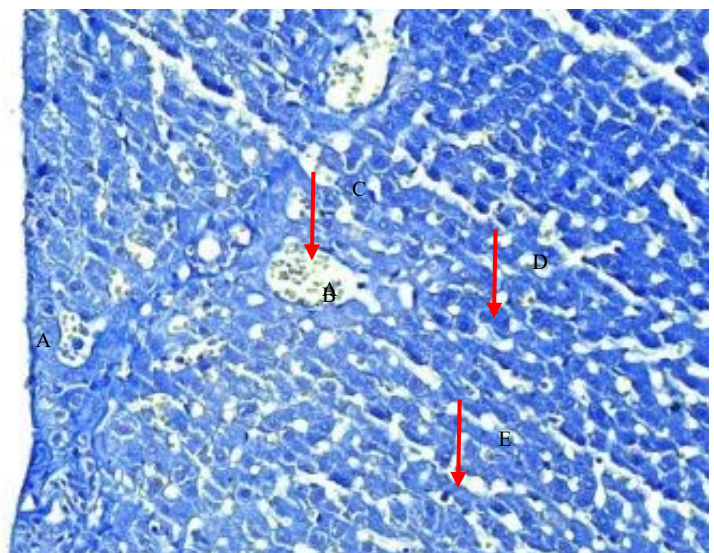


Figure 13: Liver light micrograph at 7 days of age: sinusoids (F), hepatic cells (E), hepatic duct (C), hepatic artery (D), central vein (A), endothelium (B), Verhoves, 400X.

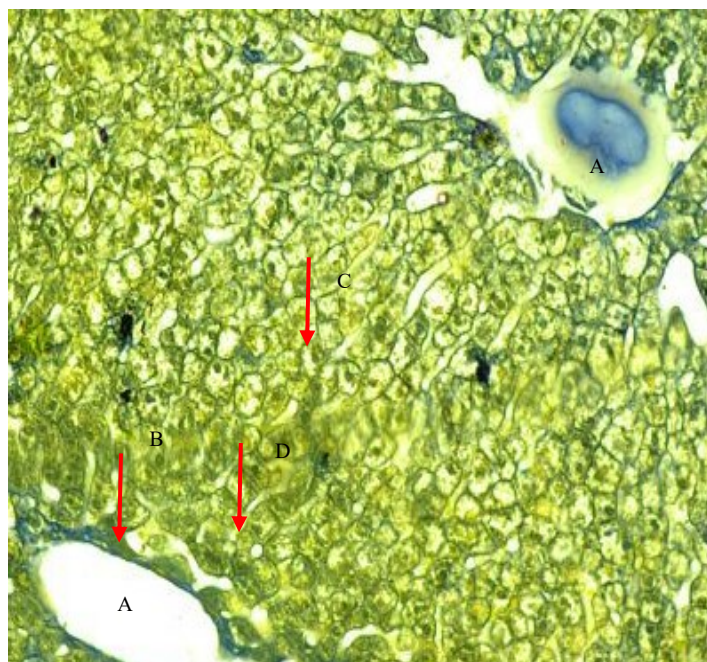


Figure 15: Liver light micrograph at 21 days of age: sinusoids (D), hepatic cells (C), endothelium (B), central vein (A), Verhoves, 400X.

Figure 14: Liver light micrograph at 14 days of age: capsule (A), sinusoids (E), hepatic cells (D), endothelium (C), central vein (B), AB, 400X.

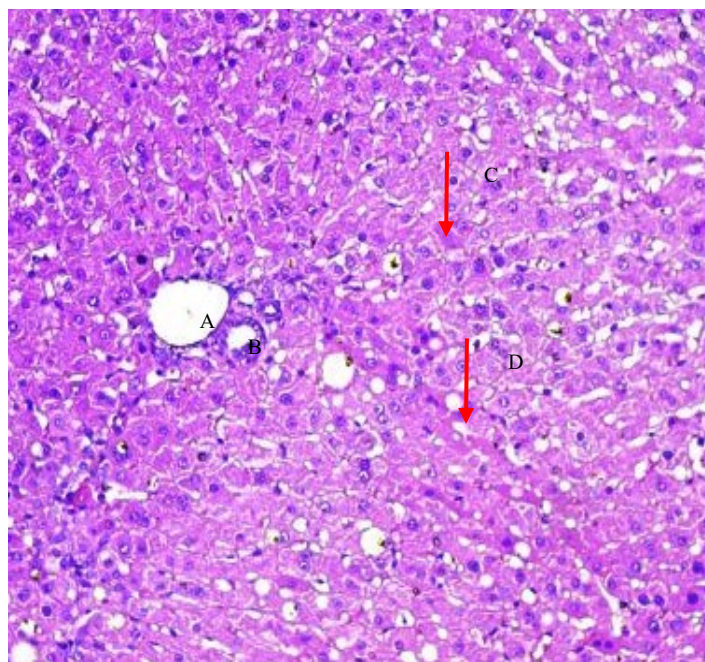


Figure 16: Liver light micrograph at 21 days of life; Masson, 400X; Hepatic cells (C), sinusoids (D), hepatic duct (B), and central vein (A).

Conclusion

As animals age, their kidneys, liver, and adrenal glands undergo structural changes. Before developing into the normal adult nephron. The liver measurements change with aging. Cortical, midcortical, and juxtamedullary renal corpuscles are distinguished by their increasing diameter with age. Distal convoluted tubules are shorter than the longest convoluted tubules, which are the proximal ones. Furthermore, Henle loops were short at one-day and adult ages but long at other ages.

Funding: No funding was received for the current work.

References

1. Y. Xing, A. M. Lerario, W. Rainey, and G. D. Hammer, "Development of adrenal cortex zonation," *Endocrinol. Metab. Clin. North Am.*, vol. 44, no. 2, pp. 243–274, 2015, doi: 10.1016/j.ecl.2015.02.001. PMID: 26038200; PMCID: PMC4486052.
2. J. Karpac, D. Ostwald, S. Bui, P. Hunnewell, M. Shankar, and U. Hochgeschwender, "Development, maintenance, and function of the adrenal gland in early postnatal proopiomelanocortin-null mutant mice," *Endocrinology*, vol. 146, no. 6, pp. 2555–2562, 2005, doi: 10.1210/en.2004-1290.
3. E. M. Elsheikh, "Histogenesis of the rabbit liver (pars hepatica) with particular reference to the portal area," *Iraqi J. Vet. Sci.*, vol. 37, no. 1, pp. 177–182, 2023.
4. N. H. Yousif, H. D. Hadi, and H. M. Jihad, "Histological study of liver in guinea pig *Cavia porcellus* (Linnaeus, 1758) in Iraq," *Rev. Bionatura*, vol. 8, no. 3, p. 80, 2023, doi: 10.21931/RB/2023.08.03.80.
5. N. H. Yousif, "Histological study of liver for squirrel (*Sciurus anomalus*) (Güldenstädt, 1785) in Iraq," *GSC Biol. Pharm. Sci.*, vol. 20, no. 1, pp. 91–94, 2022.
6. R. A. Al-Aamery et al., "Morphological description and comparative histological study of the liver in two Iraqi mammals: weasel (*Herpestes javanicus*) and eastern gray squirrel (*Sciurus carolinensis*)," *Biochem. Cell Arch.*, vol. 20, no. 1, pp. 167–170, 2020.
7. K. M. Dyce, W. O. Sack, and C. J. G. Wensing, *Textbook of Veterinary Anatomy*, 4th ed., Philadelphia: W.B. Saunders, 2010, pp. 554–694.

Indonesian Journal on Health Science and Medicine Vol 1 No 2 (2025): October

ISSN 3063-8186. Published by Universitas Muhammadiyah Sidoarjo Copyright ©
Author(s). This is an open-access article distributed under the terms of the Creative
Commons Attribution License (CC-BY).

<https://doi.org/10.21070/ijhsm.v1i2.286>

8. M. Z. Al-Hamdany, "Comparative anatomical, histological, and histochemical study of liver in human and domestic rabbit," *Iraqi J. Vet. Sci.*, vol. 33, no. 2, pp. 437–446, 2019.
9. K. Sainio, "Development of the mesonephric kidney," in C. Vize, A. S. Woolf, and J. B. L. Bard (eds.), *The Kidney: From Normal Development to Congenital Disease*, London: Academic Press, 2003, pp. 75–86.
10. W. G. Suhett, J. Gerez, M. S. Hohmann, L. Staurengo-Ferrari, W. A. Verri, and F. H. O. Pinho, et al., "Exploring porcine kidney explants as a model for the study of nephrotoxins and the therapeutic potential of phytic acid," *Environ. Toxicol. Pharmacol.*, vol. 102, p. 104241, 2023, doi: 10.1016/j.etap.104241.
11. P. Dutta, S. Hakimi, and A. T. Layton, "How the kidney regulates magnesium: a modelling study," *R. Soc. Open Sci.*, vol. 11, no. 3, p. 231484, 2024, doi: 10.1098/rsos.231484.
12. P. Kaewmong et al., "Histological study of seventeen organs from dugong (*Dugong dugon*)," *PeerJ*, vol. 11, p. e15859, 2023, doi: 10.7717/peerj.15859.
13. A. F. Baragooth, H. A. Ghazi, and K. Abdzaid, "Histological study to the nephrons of the kidney in dogs (*Canis familiaris*) in middle of Iraq," *Kufa J. Vet. Med. Sci.*, vol. 5, no. 1, pp. 98–103, 2014.
14. A. Kalita and P. C. Kalita, "Urinary system of mizo local pig (*Zovawk*): a gross morphological and histological study," *Eur. J. Biol. Pharm. Sci.*, vol. 1, no. 3, pp. 458–464, 2014.
15. M. B. Mahmood, "A comparison between ketamine-xylazine and ketamine-midazolam or all of them to induce balanced anesthesia in rabbits," *Iraqi J. Vet. Sci.*, vol. 36, no. 2, pp. 499–506, 2022, doi: 10.33899/ijvs.2021.130618.1852.
16. S. K. Suvarna, C. Layton, and J. D. Bancroft, *Bancroft's Theory and Practice of Histological Techniques*, 8th ed., Philadelphia: Churchill Livingstone Elsevier, 2018, pp. 176–725.
17. K. M. Al-Rawi and I. S. Kalaf-Allah, *Design and Analysis of Agricultural Experiments*, Mosul: Dar-Al Kutub, 1980, pp. 65, 95–107.

18. A. Plain, L. Knödl, I. Tegtmeier, et al., "The ex vivo perfused mouse adrenal gland—a new model to study aldosterone secretion," *Pflugers Arch.*, 2024, doi: 10.1007/s00424-024-02950-z.
19. T. A. Abass, "Anatomical and histological study of adrenal gland in neonatal and adult guinea pig (*Cavia porcellus*)," *Kufa J. Vet. Med. Sci.*, vol. 8, no. 1, pp. 181–192, 2017.
20. I. Ekele, N. Uchenna, and C. S. Ibe, "The kidney and adrenal gland of the African palm squirrel (*Epixerus ebii*): a microanatomical observation," *Rev. Fac. Cs. Vets.*, vol. 55, no. 2, pp. 60–67, 2014.
21. G. Rossi, K. F. Liu, H. Kershaw, D. Riddell, T. H. Hyndman, D. Monks, et al., "Biological variation in biochemistry analytes in laboratory guinea pigs (*Cavia porcellus*)," *Vet. Sci.*, vol. 10, p. 621, 2023, doi: 10.3390/vetsci10100621.
22. M. C. Nawata and T. L. Pannabecker, "Mammalian urine concentration: a review of renal medullary architecture and membrane transporters," *J. Comp. Physiol. B*, vol. 188, no. 6, pp. 899–918, 2018.
23. S. Seema, M. Rakesh, S. Sanjeev, G. B. R., and V. K., "Histological study on capsule of the kidney in large white Yorkshire pig (*Sus scrofa*)," *Indian J. Vet. Anat.*, vol. 28, no. 2, pp. 29–30, 2017.
24. I. S. Yang, I. Jang, and J. O. Yang, "CanISO: a database of genomic and transcriptomic variations in domestic dog (*Canis lupus familiaris*)," *BMC Genomics*, vol. 24, p. 613, 2023, doi: 10.1186/s12864-023-09655-0.
25. T. A. Ebeid, H. S. Aljabeili, I. H. Al-Homidan, Z. Volek, and H. Barakat, "Ramifications of heat stress on rabbit production and role of nutraceuticals in alleviating its negative impacts: an updated review," *Antioxidants*, vol. 12, no. 7, p. 1407, 2023, doi: 10.3390/antiox12071407.
26. Z. Zhou, M. J. Xu, and B. Gao, "Hepatocytes: a key cell type for innate immunity," *Cell. Mol. Immunol.*, vol. 13, pp. 301–315, 2016.